Available online at www.sciencedirect.com

SciVerse ScienceDirect

Ceramics International 38 (2012) 3635–3641

CERAMICS INTERNATIONAL

www.elsevier.com/locate/ceramint

# Lithium nickel cobalt oxides synthesized from $Li_2CO_3$, NiO and $Co_3O_4$ by the solid-state reaction method

Eui Yong Bang [a], Daniel R. Mumm [b], Hye Ryoung Park [c], Myoung Youp Song [d,*]

[a] Hanwha Chemical Research & Development Center, 6 Shinseong-Dong Yuseong-Gu, Daejeon, 305-804, Republic of Korea
[b] Department of Chemical Engineering and Materials Science, University of California Irvine, Irvine, CA 92697-2575, USA
[c] School of Applied Chemical Engineering, Chonnam National University, 300 Yongbong-Dong Buk-Gu, Gwangju, 500-757, Republic of Korea
[d] Division of Advanced Materials Engineering, Hydrogen & Fuel Cell Research Center, Engineering Research Institute, Chonbuk National University, 567 Baekje-daero Deokjin-gu, Jeonju, 561-756, Republic of Korea

Received 4 December 2011; received in revised form 25 December 2011; accepted 2 January 2012
Available online 10 January 2012

**Abstract**

$LiNi_{1-y}Co_yO_2$ ($y = 0.1$, 0.3 and 0.5) are synthesized by a solid-state reaction method at 800 °C and 850 °C from $Li_2CO_3$, NiO and $Co_3O_4$ as starting materials. The electrochemical properties of the synthesized $LiNi_{1-y}Co_yO_2$ are investigated. The synthesized $LiNi_{1-y}Co_yO_2$ has an α-$NaFeO_2$ structure with a rhombohedral system (space group; $R\bar{3}m$). Among all of the prepared $LiNi_{1-y}Co_yO_2$ ($y = 0.1$, 0.3 and 0.5) samples, $LiNi_{0.5}Co_{0.5}O_2$ calcined at 800 °C for 40 h has the best cycling performance (capacity fading rate 1.4 mAh/g/cycle) and a relatively large first discharge capacity (147.6 mAh/g). $LiNi_{0.5}Co_{0.5}O_2$ calcined at 800 °C for 40 h has a large value of $I_{0\,0\,3}/I_{1\,0\,4}$. The low degree of displacement of the nickel and lithium ions in this sample is believed to have led to its relatively large first discharge capacity and best cycling performance.


*Keywords:* $LiNi_{1-y}Co_yO_2$; Solid-state reaction method; Degree of displacement of nickel and lithium ions; Discharge capacity; Capacity fading rate

## 1. Introduction

Transition metal oxides such as $LiCoO_2$ [1–4], $LiNiO_2$ [5–12], and $LiMn_2O_4$ [13–19] have been investigated as cathode materials for lithium secondary batteries [20]. $LiMn_2O_4$ is relatively cheap and does not cause environmental pollution, but its cycling performance is poor. $LiCoO_2$ has a large diffusivity and a high operating voltage, and is easily prepared but contains an expensive element, Co.

$LiNiO_2$ is a very promising cathode material since it has a large discharge capacity [21] and is relatively excellent from the viewpoints of economics and environment. However, due to the similar sizes of Li and Ni ($Li^+ = 0.72$ Å and $Ni^{2+} = 0.69$ Å), $LiNiO_2$ is practically obtained in non-stoichiometric compositions, $Li_{1-y}Ni_{1+y}O_2$ [22,23], and the $Ni^{2+}$ ions in the lithium planes obstruct the movement of the $Li^+$ ions during charge and discharge [24,25].

The drawbacks of $LiCoO_2$ and $LiNiO_2$ can be overcome by incorporating phases with $LiNi_{1-y}Co_yO_2$ compositions because the presence of cobalt stabilizes the structure in a strictly two-dimensional fashion, thus favoring good reversibility of the intercalation and deintercalation reactions [24,26–33]. Rougier et al. [24] reported that the stabilization of the two-dimensional character of the structure by cobalt substitution in $LiNiO_2$ is correlated with an increase in the cell performance due to a decrease in the amount of extra-nickel ions in the inter-slab space which impede the lithium diffusion.

In this work, $LiNi_{1-y}Co_yO_2$ ($y = 0.1$, 0.3and 0.5) cathode materials were synthesized by a solid-state reaction method at different temperatures using $Li_2CO_3$, NiO and $Co_3O_4$ as starting materials. The electrochemical properties of the synthesized samples were then investigated.

## 2. Experimental

$Li_2CO_3$ (High Purity Chemical Laboratory Co., purity 99 %), NiO (High Purity Chemical Laboratory Co., purity 99.9 %) and $Co_3O_4$ (High Purity Chemical Laboratory Co., purity 99.9 %)

* Corresponding author. Tel.: +82 63 270 2379; fax: +82 63 270 2386.
*E-mail address:* songmy@jbnu.ac.kr (M.Y. Song).

0272-8842/$36.00 
doi:10.1016/j.ceramint.2012.01.002

were used as starting materials in order to synthesize $LiNi_{1-y}Co_yO_2$ by the solid-state reaction method.

The experimental procedure is shown schematically in Fig. 1. Starting materials with the compositions of $LiNi_{1-y}Co_yO_2$ ($y = 0.1, 0.3$ and 0.5) were mixed and pelletized. These pellets were heat-treated in air at 650 °C for 20 h, and were ground, mixed, and pelletized again. They were then calcined at 800 °C or 850 °C for 20 h. Pellets were cooled at a cooling rate of 50 °C/min, ground, mixed and pelletized again. They were then calcined again at 800 °C or 850 °C for 20 h.

Phase identification of the synthesized samples was carried out by X-ray diffraction (XRD) analysis with Cu Kα radiation using a Rigaku type III/A X-ray diffractometer. The scanning rate was 4°/min and the scanning range of the diffraction angle ($2\theta$) was $10^\circ \leq 2\theta \leq 70^\circ$. Morphologies of the samples were observed using a field emission scanning electron microscope (FE-SEM). The particle size distributions and the specific surface areas of the samples were analyzed by a particle size analyzer (Malvern Instruments).

The electrochemical cells consisted of $LiNi_{1-y}Co_yO_2$ as a cathode, Li foil as an anode, and an electrolyte (Purelyte, Samsung Chemicals Ltd.) prepared by dissolving 1 M $LiPF_6$ in a 1:1 (volume ratio) mixture of ethylene carbonate (EC) and dimethyl carbonate (DMC). A Whatman glass-fiber was used as the separator. To fabricate the cathode, 89 wt% synthesized $LiNi_{1-y}Co_yO_2$, 10 wt% acetylene black and 1 wt% polytetrafluoroethylene (PTFE) binder were mixed in an agate mortar. The cell was assembled in a glove box filled with argon. All of the electrochemical tests were performed at room temperature with a potentiostatic/galvanostatic system. The cells were cycled at a current density of 200 μA/cm$^2$ between 3.2 and 4.3 V.

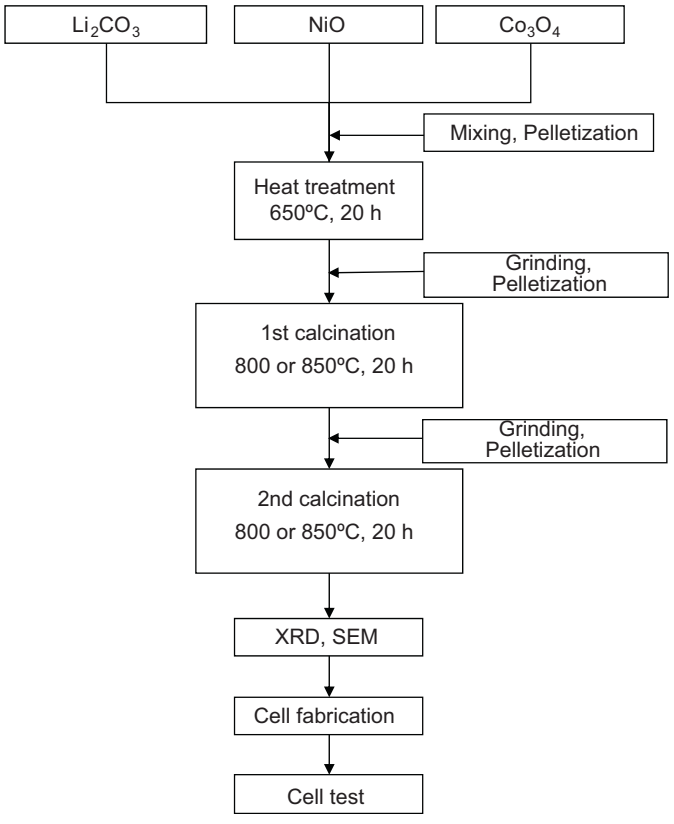


Fig. 1. Experimental procedure to synthesized $LiNi_{1-y}Co_yO_2$ ($y = 0.1, 0.3$ and 0.5) by the solid-state reaction method from $Li_2CO_3$, NiO and $Co_3O_4$.

## 3. Results and discussion

Fig. 2 shows the XRD patterns of $LiNi_{1-y}Co_yO_2$ ($y = 0.1$, 0.3 and 0.5) powders from $Li_2CO_3$, NiO and $Co_3O_4$ calcined at 800 °C for 20 h. They correspond to an α-$NaFeO_2$ structure with a rhombohedral system (space group; $R\bar{3}m$). Impurity peaks appear at diffraction angles $2\theta = 21^\circ$ and 32°. These peaks are identified as those of the $Li_2CO_3$ phase. As the Co content increases, the intensities of these peaks decrease.

XRD patterns of $LiNi_{1-y}Co_yO_2$ ($y = 0.1$, 0.3 and 0.5) powders from $Li_2CO_3$, NiO and $Co_3O_4$ calcined at 800 °C for 40 h are exhibited in Fig. 3. They also show the phase with the α-$NaFeO_2$ structure of the rhombohedral system (space group: $R\bar{3}m$). As the Co content increases, the intensities of the peaks of the $Li_2CO_3$ phase appearing at diffraction angles $2\theta = 21^\circ$ and 32° decrease quite rapidly, and are extremely weak in the

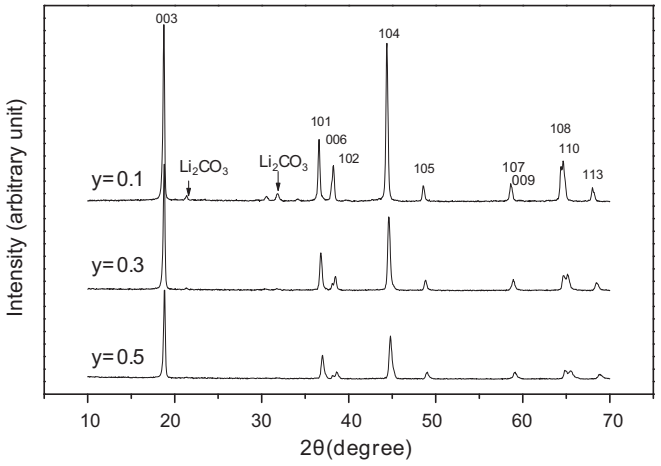


Fig. 2. XRD patterns of $LiNi_{1-y}Co_yO_2$ ($y = 0.1$, 0.3 and 0.5) powders calcined at 800 °C for 20 h.

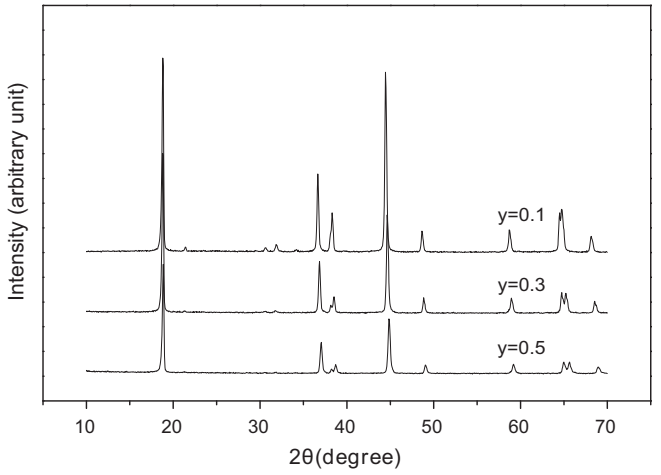


Fig. 3. XRD patterns of $LiNi_{1-y}Co_yO_2$ ($y = 0.1$, 0.3 and 0.5) powders synthesized at 800 °C for 40 h.

$LiNi_{0.5}Co_{0.5}O_2$ sample. Peaks of the $Li_2CO_3$ phase become weaker compared with those in Fig. 2. In Figs. 2 and 3, the relative intensity of the 0 0 3 peak compared to that of the 1 0 4 peak increases and the splitting of the (1 0 8) and (1 1 0) lines becomes clearer as the Co content increases.

The fraction of each phase from the intensity ratios of the 0 0 3 and 1 0 4 peaks can be calculated since the 0 0 3 peak originates from the diffraction of only the $R\bar{3}m$ α-$NaFeO_2$ structure while the 1 0 4 peak originates from the diffractions of both the $R\bar{3}m$ α-$NaFeO_2$ and $Fm\bar{3}m$ NaCl structures. The intensity ratios of the 0 03 and 1 0 4 peaks, $I_{0\,0\,3}/I_{1\,0\,4}$, of the completely stoichiometric composition $LiNiO_2$ was reported to be about 1.3 by Morales et al. [34]. Ohzuku et al. [35] reported that the intensity ratio of the 0 0 3 and 1 0 4 peaks is a key parameter of the degree of displacement of the nickel and lithium ions. As the intensity ratio of the 0 0 3 and 1 0 4 peaks increases, the degree of displacement of the nickel and lithium ions decreases. They also reported that electroactive $LiNiO_2$ showed a clear split of the (1 0 8) and (1 1 0) lines, which appear in their XRD patterns at a diffraction angle near $2\theta = 65^\circ$.

The variation of the intensity ratio of 0 0 3 and 1 0 4 peaks, $I_{0\,0\,3}/I_{1\,0\,4}$, with $y$ in $LiNi_{1-y}Co_yO_2$ calcined at 800 °C for 20 h and 40 h is presented in Fig. 4. As the value of $y$ increases, the value of $I_{0\,0\,3}/I_{1\,0\,4}$ increases. As calcination time increases, the value of $I_{0\,0\,3}/I_{1\,0\,4}$ increases for the same compositions. The $I_{0\,0\,3}/I_{1\,0\,4}$ values of $LiNi_{0.5}Co_{0.5}O_2$ calcined for 20 h, $LiNi_{0.7}Co_{0.3}O_2$ calcined for 40 h, and $LiNi_{0.5}Co_{0.5}O_2$ calcined for 40 h are 1.331, 1.341 and 1.410, respectively, indicating that the composition of these samples is stoichiometric. These show that as the Co content and the calcination time increase, the degree of displacement of the nickel and lithium ions decreases. Figs. 2 and 3 show that the splitting of the (1 0 8) and (1 1 0) lines becomes clearer as the Co content increases. The XRD patterns of $LiNi_{1-y}Co_yO_2$ ($y = 0.1$, 0.3 and 0.5) powders from $Li_2CO_3$, NiO and $Co_3O_4$ calcined at 850 °C for 40 h showed that they were very similar to those of $LiNi_{1-y}Co_yO_2$ ($y = 0.1$, 0.3 and 0.5) powders calcined at 800 °C for 40 h, the $Li_2CO_3$ peaks being weaker.

The intensity ratio, $R$, was defined by Dahn et al. [7] as the relative intensity of the (1 0 2, 0 0 6) Bragg peak near $2\theta = 38^\circ$ as compared with that of the 1 0 1 peak near $2\theta = 36.5^\circ$. Their results showed that the intensity ratio, $R$, increases as the unit cell volume increases. They also showed that the intensity ratio, $R$, increases rapidly as $x$ decreases in $Li_xNi_{2-x}O_2$. This suggests that, as the unit cell volume increases, $x$ decreases in $Li_xNi_{2-x}O_2$, which can be expressed as $(Li_xNi_{1-x})NiO_2$. A decrease in $x$ in $Li_xNi_{2-x}O_2$ corresponds to an increase in the degree of displacement of the nickel and lithium ions. The variations of unit cell volume with $y$ in $LiNi_{1-y}Co_yO_2$ calcined at 800 and 850 °C for 40 h are given in Fig. 5. As the value of $y$ increases, the unit cell volume decreases. This shows that as the Co content increases, the degree of displacement of the nickel and lithium ions decreases.

Variations of the parameters of the hexagonal unit cell, $a$ and $c$, and the degree of trigonal distortion, $c/a$, with $y$ in $LiNi_{1-y}Co_yO_2$ calcined at 800 °C for 40 h are shown in Fig. 6. As the Co content increases, the lattice parameters $a$ and c decrease. The reason for this is that the radius of the Co ion [0.53 Å (low spin)] is smaller than that of the Ni ion [0.60 Å (low spin)]. The value of $c/a$ increases as $y$ increases from 0.1 to 0.5. The increase in the value of $c/a$ signifies better development of the two-dimensional structure.

Fig. 7 presents SEM micrographs of $LiNi_{1-y}Co_yO_2$ ($y = 0.1$, 0.3 and 0.5) calcined at 800 °C for 20 h. The samples consist of small and large particles. The particle size difference between small particles and large ones is quite large. The shapes of the particles are irregular. Some particles are agglomerated with small particles.

FE-SEM micrographs of $LiNi_{1-y}Co_yO_2$ ($y = 0.1$, 0.3 and 0.5) calcined at 800 °C for 40 h are presented in Fig. 8. The samples consist of small and large particles. The particle size of the larger particles becomes larger as the Co content increases from $y = 0.1$ to $y = 0.3$, and then decreases from $y = 0.3$ to

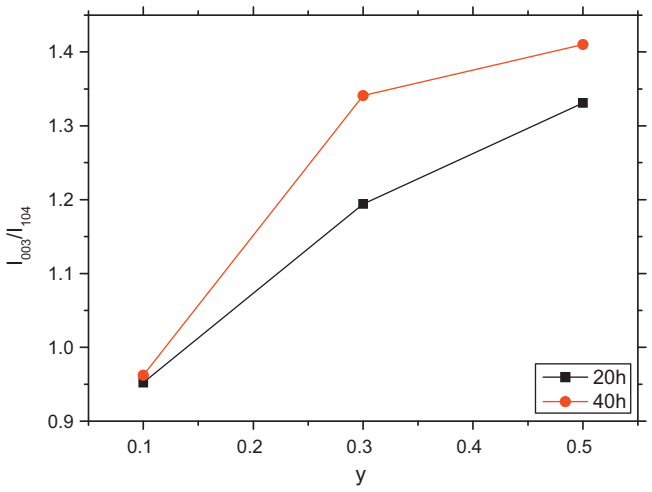


Fig. 4. Variation of intensity ratio of 0 0 3 and 1 0 4 peaks, $I_{0\,0\,3}/I_{1\,0\,4}$, with $y$ in $LiNi_{1-y}Co_yO_2$ calcined at 800 °C for 20 and 40 h.

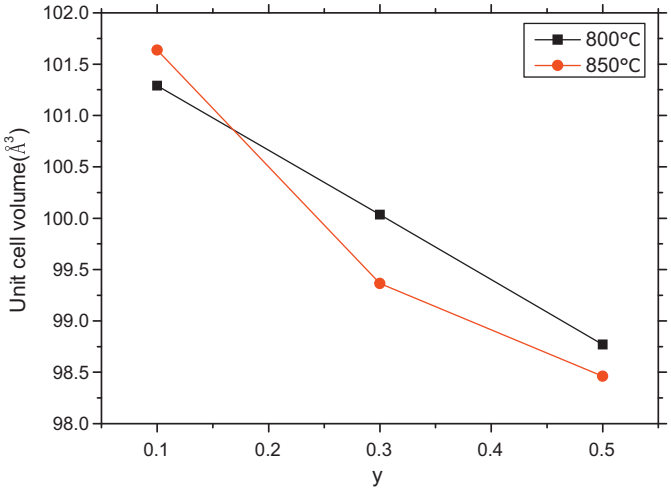


Fig. 5. Variation of unit cell volume with $y$ in $LiNi_{1-y}Co_yO_2$ calcined at 800 and 850 °C for 40 h.

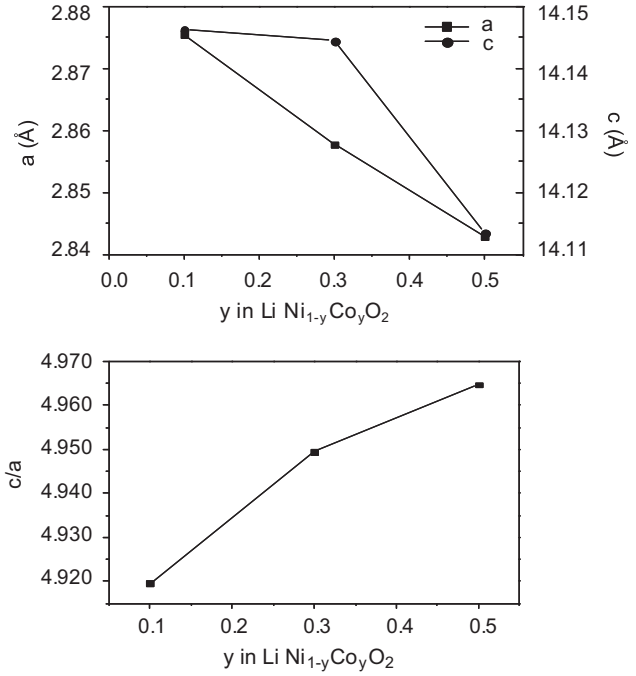


Fig. 6. Variations of lattice parameter $a$, $c$ and their ratio $c/a$ with $y$ in $LiNi_{1-y}Co_yO_2$ synthesized at 800 °C for 40 h.

$y = 0.5$. On the whole, $LiNi_{0.7}Co_{0.3}O_2$ has the largest particle size, followed in order by $LiNi_{0.5}Co_{0.5}O_2$ and $LiNi_{0.9}Co_{0.1}O_2$. Compared with the microstructures of $LiNi_{1-y}Co_yO_2$ ($y = 0.1$, 0.3 and 0.5) calcined for 20 h in Fig. 7, the particle sizes were more homogeneous.

Fig. 9 shows the FE-SEM micrographs of $LiNi_{1-y}Co_yO_2$ ($y = 0.1$, 0.3 and 0.5) calcined at 850 °C for 40 h. The samples consist of small and large particles. $LiNi_{0.9}Co_{0.1}O_2$ has particles with uneven surfaces and sharp edges. In the $LiNi_{0.7}Co_{0.3}O_2$ sample, particles with flat surfaces appear. In the $LiNi_{0.5}Co_{0.5}O_2$ sample, all the particles have flat surfaces and rounded edges. The particles are larger than those of the samples in Fig. 8.

Variations in discharge capacity at 200 μA/cm$^2$ with the number of cycles ($n$) for $LiNi_{1-y}Co_yO_2$ ($y = 0.1$, 0.3 and 0.5) calcined at 800 °C for 40 h are presented in Fig. 10. $LiNi_{0.7}Co_{0.3}O_2$ has the largest first discharge capacity of 153.8 mAh/g, followed in order by $LiNi_{0.5}Co_{0.5}O_2$ (147.6 mAh/g) and $LiNi_{0.9}Co_{0.1}O_2$ (122.1 mAh/g). $LiNi_{0.5}Co_{0.5}O_2$ has the best cycling performance with a discharge capacity of 139.3 mAh/g at $n = 7$, followed in order by $LiNi_{0.9}Co_{0.1}O_2$ (90.5 mAh/g at $n = 7$) and $LiNi_{0.7}Co_{0.3}O_2$ (107.3 mAh/g at $n = 7$). The discharge capacity fading rates are calculated using all the data from $n = 1$ to $n = 7$, and are 5.4, 7.3, and 1.4 mAh/g/cycle, respectively, for the samples $LiNi_{1-y}Co_yO_2$ ($y = 0.1$, 0.3 and 0.5).

Fig. 11 shows the variations in discharge capacity at 200 μA/cm$^2$ as a function of the number of cycles for

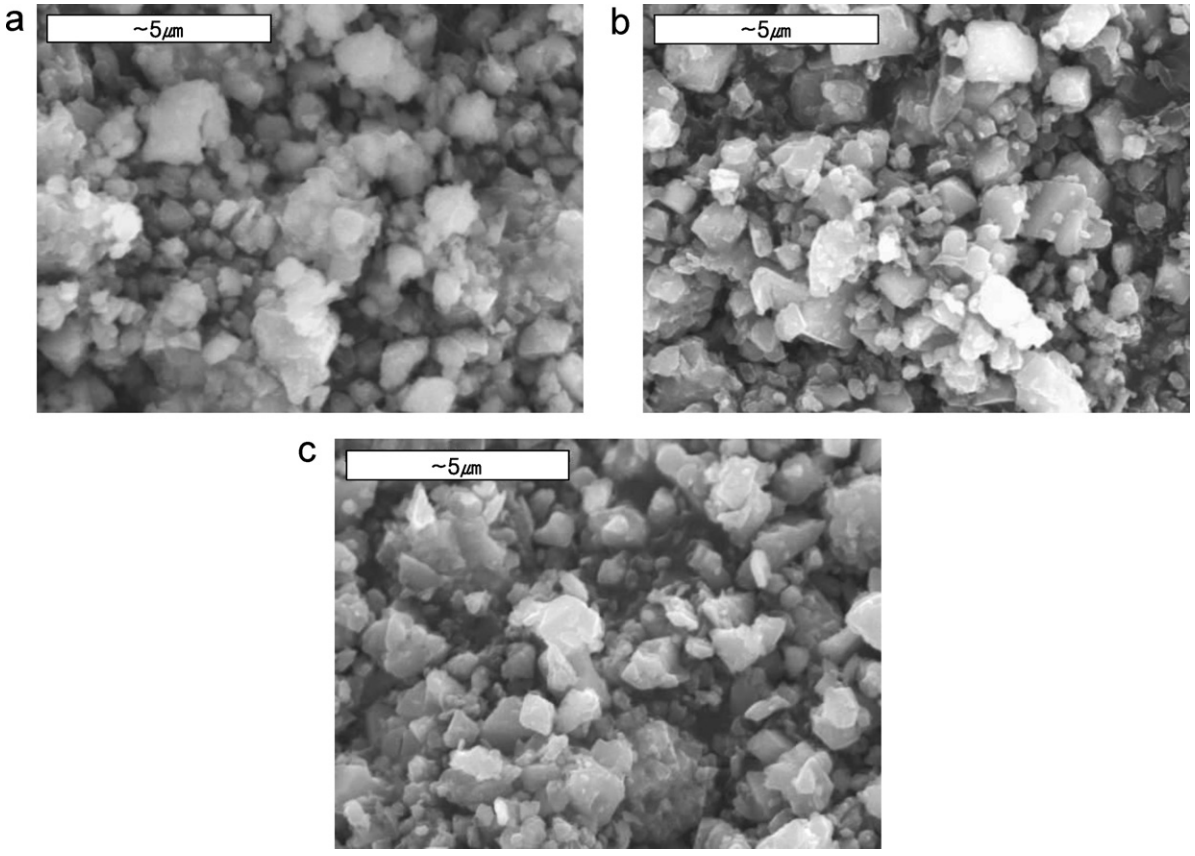


Fig. 7. SEM micrographs of $LiNi_{1-y}Co_yO_2$ calcined at 800 °C for 20 h from $Li_2CO_3$, NiO and $Co_3O_4$; (a) $y = 0.1$, (b) $y = 0.3$ and (c) $y = 0.5$.

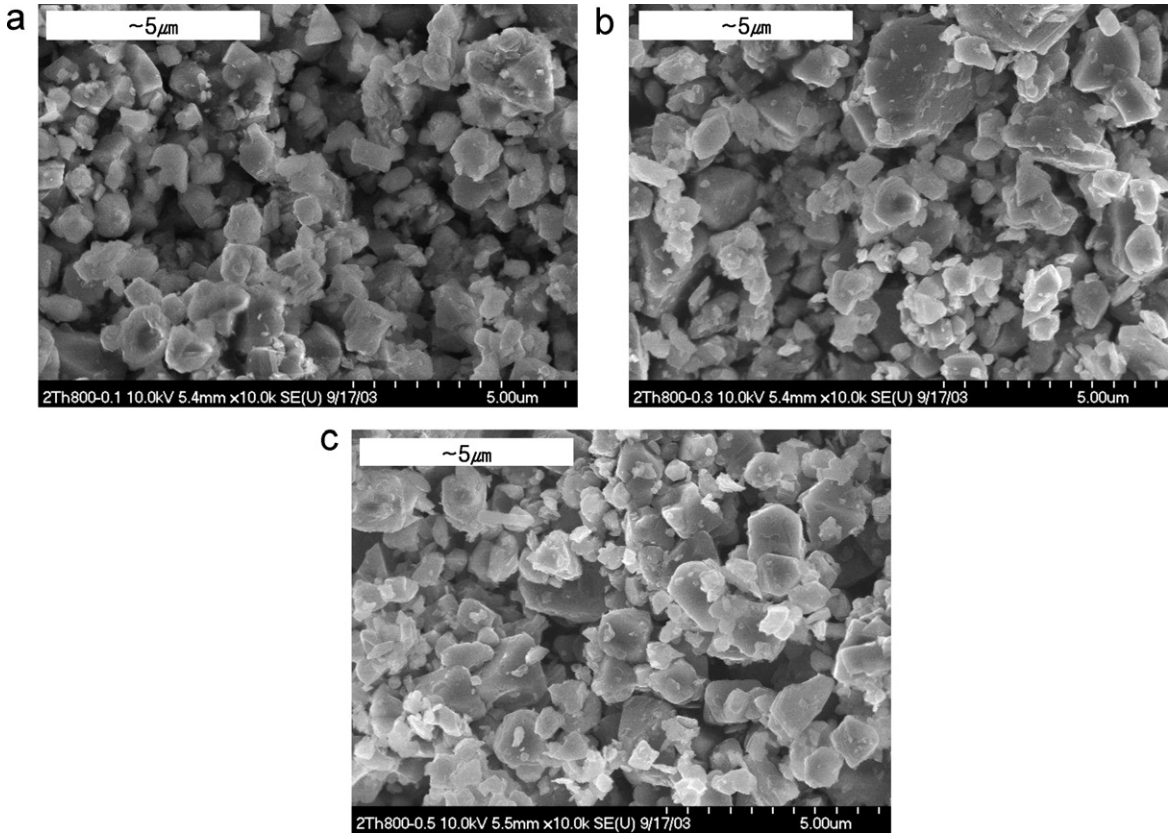


Fig. 8. FE-SEM micrographs of $LiNi_{1-y}Co_yO_2$ calcined at 800 °C for 40 h; (a) $y = 0.1$, (b) $y = 0.3$ and (c) $y = 0.5$.

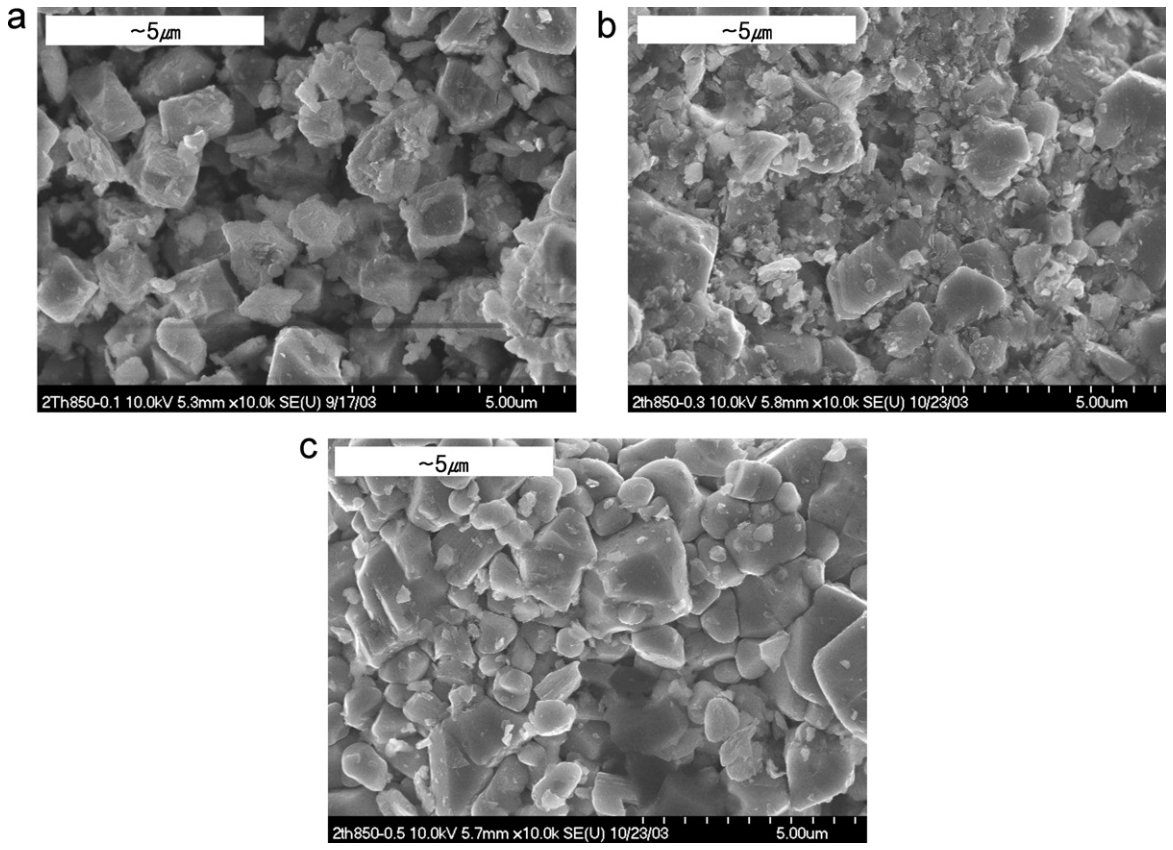


Fig. 9. FE-SEM micrographs of $LiNi_{1-y}Co_yO_2$ calcined at 850 °C for 40 h; (a) $y = 0.1$, (b) $y = 0.3$ and (c) $y = 0.5$.

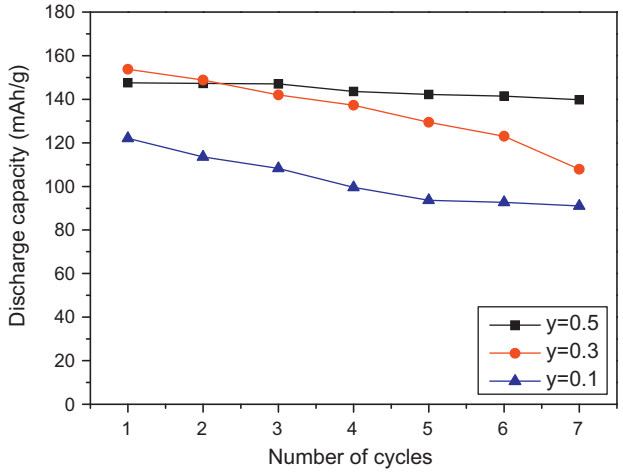


Fig. 10. Variations of discharge capacity at 200 μA/cm$^2$ with the number of cycles for $LiNi_{1-y}Co_yO_2$ calcined at 800 °C for 40 h.

$LiNi_{1-y}Co_yO_2$ ($y = 0.1$, 0.3 and 0.5) calcined at 850 °C for 40 h. $LiNi_{0.5}Co_{0.5}O_2$ has the largest first discharge capacity of 149.2 mAh/g, followed in order by $LiNi_{0.9}Co_{0.1}O_2$ (119.5 mAh/g) and $LiNi_{0.7}Co_{0.3}O_2$ (109.0 mAh/g). All of the samples have poor cycling performance. $LiNi_{1-y}Co_yO_2$ ($y = 0.1$, 0.3 and 0.5) have discharge capacities of 78.5, 54.4, and 114.1 mAh/g, respectively, at $n = 7$. The discharge capacity fading rates are 6.6, 10.0, and 5.5 mAh/g/cycle, respectively, for $LiNi_{1-y}Co_yO_2$ ($y = 0.1$, 0.3 and 0.5). $LiNi_{0.5}Co_{0.5}O_2$ has the best cycling performance, followed in order by $LiNi_{0.9}Co_{0.1}O_2$ and $LiNi_{0.7}Co_{0.3}O_2$.

Fig. 10 shows that $LiNi_{0.5}Co_{0.5}O_2$ has the best cycling performance (capacity fading rate 1.4 mAh/g/cycle) among the samples calcined at 800 °C for 40 h and a relatively large first discharge capacity (147.6 mAh/g). Fig. 11 shows that $LiNi_{0.5}Co_{0.5}O_2$ has the largest first discharge capacity (149.2 mAh/g) and the best cycling performance (even though it has poor cycling performance) among the samples calcined at 850 °C for 40 h. In Fig. 4, $LiNi_{0.5}Co_{0.5}O_2$ calcined for 40 h has the largest value of $I_{0\,0\,3}/I_{1\,0\,4}$ among the samples calcined at

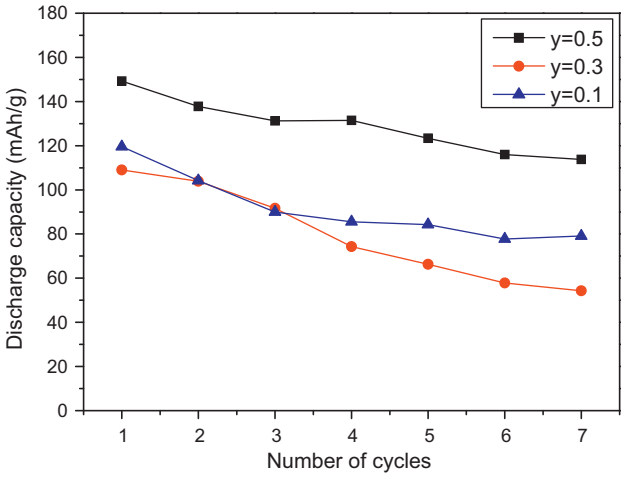


Fig. 11. Variations in discharge capacity at 200 μA/cm$^2$ with the number of cycles for $LiNi_{1-y}Co_yO_2$ calcined at 850 °C for 40 h.

800 °C, and in Fig. 5, $LiNi_{0.5}Co_{0.5}O_2$ calcined at 850 °C has the smallest unit cell volume ($LiNi_{0.5}Co_{0.5}O_2$ calcined at 800 °C has the second smallest unit cell volume) among the samples calcined at 800 °C and 850 °C for 40 h, showing that the $LiNi_{0.5}Co_{0.5}O_2$ samples calcined at 800 °C and 850 °C for 40 h have low degree of displacement of nickel and lithium ions. The low degree of displacement of the nickel and lithium ions in these samples is believed to result in their relatively large first discharge capacities and best cycling performance.

## 4. Conclusions

$LiNi_{1-y}Co_yO_2$ ($y = 0.1$, 0.3 and 0.5) are synthesized by the solid-state reaction method at 800 °C and 850 °C from $Li_2CO_3$, NiO and $Co_3O_4$. $LiNi_{1-y}Co_yO_2$ has an α-$NaFeO_2$ structure with a rhombohedral system (space group; $R\bar{3}m$). As the Co content increases, the intensities of $Li_2CO_3$ impurity peaks decrease quite rapidly, and they are extremely weak in the $LiNi_{0.5}Co_{0.5}O_2$ sample. As the Co content increases, the relative intensity of the 0 0 3 peak compared to that of the 1 0 4 peak increases. Among all of the prepared $LiNi_{1-y}Co_yO_2$ ($y = 0.1$, 0.3 and 0.5) samples, $LiNi_{0.5}Co_{0.5}O_2$ calcined at 800 °C for 40 h has the best cycling performance (capacity fading rate 1.4 mAh/g/cycle) and a relatively large first discharge capacity (147.6 mAh/g). $LiNi_{0.5}Co_{0.5}O_2$ calcined at 800 °C for 40 h has a large value of $I_{0\,0\,3}/I_{1\,0\,4}$. The low degree of displacement of the nickel and lithium ions in this sample is believed to have led to its relatively large first discharge capacity and best cycling performance. As the Co content increases, the lattice parameters $a$ and $c$ decrease and the value of $c/a$ increases.

## References

[1] K. Ozawa, Lithium-ion rechargeable batteries with $LiCoO_2$ and carbon electrodes: the $LiCoO_2$/C system, Solid State Ionics 69 (1994) 212–221.
[2] R. Alcántara, P. Lavela, J.L. Tirado, R. Stoyanova, E. Zhecheva, Structure and electrochemical properties of boron-doped $LiCoO_2$, J. Solid State Chem. 134 (1997) 265–273.
[3] Z.S. Peng, C.R. Wan, C.Y. Jiang, Synthesis by sol–gel process and characterization of $LiCoO_2$ cathode materials, J. Power Sources 72 (1998) 215–220.
[4] W.D. Yang, C.Y. Hsieh, H.J. Chuang, Y.S. Chen, Preparation and characterization of nanometric-sized $LiCoO_2$ cathode materials for lithium batteries by a novel sol–gel method, Ceram. Int. 36 (1) (2010) 135–140.
[5] C.H. Han, J.H. Kim, S.H. Paeng, D.J. Kwak, Y.M. Sung, Electrochemical characteristics of $LiNiO_2$ films prepared for charge storable electrode application, Thin Solid Films 517 (14) (2009) 4215–4217.
[6] S.N. Kwon, J.H. Song, D.R. Mumm, Effects of cathode fabrication conditions and cycling on the electrochemical performance of $LiNiO_2$ synthesized by combustion and calcination, Ceram. Int. 37 (5) (2011) 1543–1548.
[7] J.R. Dahn, U. von Sacken, C.A. Michal, Structure and electrochemistry of $Li_{1\pm y}NiO_2$ and a new $Li_2NiO_2$ phase with the Ni $(OH)_2$ structure, Solid State Ionics 44 (1990) 87–97.
[8] J.R. Dahn, U. von Sacken, M.W. Juzkow, H. Al-Janaby, Rechargeable $LiNiO_2$/carbon cells, J. Electrochem. Soc. 138 (1991) 2207–2212.
[9] H.U. Kim, D.R. Mumm, H.R. Park, M.Y. Song, Synthesis by a simple combustion method and electrochemical properties of $LiCo_{1/3}Ni_{1/3}Mn_{1/3}O_2$, Electron. Mater. Lett. 6 (3) (2010) 91–95.
[10] S.H. Ju, J.H. Kim, Y.C. Kang, Electrochemical properties of $LiNi_{0.8}Co_{0.2-x}Al_xO_2$ ($0 \le x \le 0.1$) cathode particles prepared by spray pyrolysis

from the spray solutions with and without organic additives, Met. Mater. Int. 16 (2) (2010) 299–303.
[11] D.H. Kim, Y.U. Jeong, Crystal structures and electrochemical properties of $LiNi_{1-x}Mg_xO_2$ ($0 \leq x \leq 0.1$) for cathode materials of secondary lithium batteries, Korean J. Met. Mater. 48 (3) (2010) 262–267.
[12] M.Y. Song, D.R. Mumm, C.K. Park, H.R. Park, Cycling performances of $LiNi_{1-y}M_yO_2$ (M = Ni, Ga, Al and/or Ti) synthesized by wet milling and solid-state method, Met. Mater. Int., in press.
[13] A.R. Armstrong, P.G. Bruce, Synthesis of layered $LiMnO_2$ as an electrode for rechargeable lithium batteries, Lett. Nat. 381 (1996) 499–500.
[14] J.M. Tarascon, E. Wang, F.K. Shokoohi, W.R. Mckinnon, S. Colson, The spinel phase of $LiMn_2O_4$ as a cathode in secondary lithium cells, J. Electrochem. Soc. 138 (1991) 2859–2864.
[15] M.Y. Song, D.S. Ahn, On the capacity deterioration of spinel phase $LiMn_2O_4$ with cycling around 4 V, Solid State Ionics 112 (1998) 21–24.
[16] M.Y. Song, D.S. Ahn, H.R. Park, Capacity fading of spinel phase $LiMn_2O_4$ with cycling, J. Power Sources 83 (1999) 57–60.
[17] D.S. Ahn, M.Y. Song, Variations of the electrochemical properties of $LiMn_2O_4$ with synthesis conditions, J. Electrochem. Soc. 147 (3) (2000) 874–879.
[18] H.J. Guo, Q.H. Li, X.H. Li, Z.X. Wang, W.J. Peng, Novel synthesis of $LiMn_2O_4$ with large tap density by oxidation of manganese powder, Energy Convers. Manage. 52 (4) (2011) 2009–2014.
[19] C. Wan, M. Cheng, D. Wu, Synthesis of spherical spinel $LiMn_2O_4$ with commercial manganese carbonate, Powder Technol. 210 (1) (2011) 47–51.
[20] J.W. Park, J.H. Yu, K.W. Kim, H.S. Ryu, J.H. Ahn, C.S. Jin, K.H. Shin, Y.C. Kim, H.J. Ahn, Surface morphology changes of lithium/sulfur battery using multi-walled carbon nanotube added sulfur electrode during cyclings, Korean J. Met. Mater. 49 (2) (2011) 174–179.
[21] Y. Nishida, K. Nakane, T. Satoh, Synthesis and properties of gallium-doped $LiNiO_2$ as the cathode material for lithium secondary batteries, J. Power Sources 68 (1997) 561–564.
[22] P. Barboux, J.M. Tarascon, F.K. Shokoohi, The use of acetates as precursors for the low-temperature synthesis of $LiMn_2O_4$ and $LiCoO_2$ intercalation compounds, J. Solid State Chem. 94 (1991) 185–196.
[23] J. Morales, C. Perez-Vicente, J.L. Tirado, Cation distribution and chemical deintercalation of $Li_{1-x}Ni_{1+x}O_2$, Mater. Res. Bull. 25 (1990) 623–630.
[24] A. Rougier, I. Saadoune, P. Gravereau, P. Willmann, C. Delmas, Solid State Ionics 90 (1996) 83–90.
[25] B.J. Neudecker, R.A. Zuhr, B.S. Kwak, J.B. Bates, J.D. Robertson, Lithium manganese nickel oxides $Li_x(Mn_yNi_{1-y})_{2-x}O_2$, J. Electrochem. Soc. 145 (1998) 4148–4157.
[26] C. Delmas, I. Saadoune, Electrochemical and physical properties of the $Li_xNi_{1-y}Co_yO_2$ phases, Solid State Ionics 53–56 (1992) 370–375.
[27] E. Zhecheva, R. Stoyanova, Stabilization of the layered crystal structure of $LiNiO_2$ by Co-substitution, Solid State Ionics 66 (1993) 143–149.
[28] C. Delmas, I. Saadoune, A. Rougier, The cycling properties of the $Li_xNi_{1-y}Co_yO_2$ electrode, J. Power Sources 43–44 (1993) 595–602.
[29] A. Ueda, T. Ohzuku, Solid-state redox reactions of $LiNi_{1/2}Co_{1/2}O_2$ ($R\bar{3}m$) for 4 volt secondary lithium cells, J. Electrochem. Soc. 141 (1994) 2010–2014.
[30] M. Menetrier, A. Rougier, C. Delmas, Cobalt segregation in the $LiNi_{1-y}Co_yO_2$ solid solution: a preliminary $^7Li$ NMR study, Solid State Commun. 90 (1994) 439–442.
[31] R. Alcantara, J. Morales, J.L. Tirado, R. Stoyanova, E. Zhecheva, Structure and electrochemical properties of $Li_{1-x}(Ni_yCo_{1-y})_{1+x}O_2$. Effect of chemical delithiation at 0 °C, J. Electrochem. Soc. 142 (1995) 3997–4005.
[32] E. Levi, M.D. Levi, G. Salitra, D. Aurbach, R. Oesten, U. Heider, L. Heider, Electrochemical and in situ XRD characterization of $LiNiO_2$ and $2LiCo_{0.2}Ni_{0.8}O_2$ electrodes for rechargeable lithium cells, Solid State Ionics 126 (1999) 97–108.
[33] M.Y. Song, J. Song, E.Y. Bang, D.R. Mumm, Electrochemical properties of $LiNi_{1-y}Co_yO_2$ cathode materials synthesized from different starting materials by the solid-state reaction method, Ceram. Int. 35 (2009) 1625–1631.
[34] J. Morales, C. Pérez-Vicente, J.L. Tirado, Cation distribution and chemical deintercalation of $Li_{1-x}Ni_{1+x}O_2$, Mater. Res. Bull. 25 (1990) 623–630.
[35] T. Ohzuku, A. Ueda, M. Nagayama, Electrochemistry and structural chemistry of $LiNiO_2$ ($R\bar{3}m$) for 4 volt secondary lithium cells, J. Electrochem. Soc. 140 (1993) 1862–1870.